

VU Research Portal

Enzymatic Activity and Excited State Processes in Protochlorophyllide Oxidoreductase

Sytina, O.

2010

document version

Publisher's PDF, also known as Version of record

[Link to publication in VU Research Portal](#)

citation for published version (APA)

Sytina, O. (2010). *Enzymatic Activity and Excited State Processes in Protochlorophyllide Oxidoreductase*.

General rights

Copyright and moral rights for the publications made accessible in the public portal are retained by the authors and/or other copyright owners and it is a condition of accessing publications that users recognise and abide by the legal requirements associated with these rights.

- Users may download and print one copy of any publication from the public portal for the purpose of private study or research.
- You may not further distribute the material or use it for any profit-making activity or commercial gain
- You may freely distribute the URL identifying the publication in the public portal ?

Take down policy

If you believe that this document breaches copyright please contact us providing details, and we will remove access to the work immediately and investigate your claim.

E-mail address:

vuresearchportal.ub@vu.nl

~ CHAPTER 5 ~

**Protochlorophyllide Excited State Dynamics in Organic Solvents
Studied by Time-Resolved Visible and Mid-IR Spectroscopy**

Olga A. Sytina, Ivo H.M. van Stokkum, Derren J. Heyes, C. Neil Hunter, Rienk van Grondelle and Marie Louise Groot

Protochlorophyllide (Pchl_{id}) is a precursor in the biosynthesis of chlorophyll. Complexed with NADPH to the enzyme protochlorophyllide oxidoreductase (POR), it is reduced to chlorophyllide, a process that occurs via a set of spectroscopically distinct intermediate states, and is initiated from the excited state of Pchl_{id}. To obtain a better understanding of these catalytic events, we characterized the excited state dynamics of Pchl_{id} in the solvents tetrahydrofuran (THF), methanol and Tris/Triton buffer, using ultrafast transient absorption in the visible and midinfrared spectral regions, and time-resolved fluorescence emission experiments. For comparison, we present time-resolved transient absorption measurements of chlorophyll *a* in THF. From the combined analysis of these experiments, we derive that during the 2-3 ns excited state lifetime an extensive multiphasic quenching of the emission occurs, due to solvation of the excited state, in agreement with the previously proposed internal charge-transfer (ICT) character of the S₁ state⁽⁴¹⁾. The solvation process in methanol occurs in conjunction with a strengthening of a hydrogen bond to the Pchl_{id} keto carbonyl group. We demonstrate that the internal conversion from the S₂ to S₁ excited states is remarkably slow, and stretches out on to the 700 fs timescale, causing a rise of blue-shifted signals in the transient absorption, and a gain of emission in the time-resolved fluorescence. A triplet state is populated on the nanosecond timescale with a maximal yield of ~23%. The consequences of these observations for the catalytic pathway and the role of the triplet and ICT state in activation of the enzyme are discussed.

submitted to *The Journal of Physical Chemistry B*

5.1. Introduction

Protochlorophyllide (Pchl)ide is a porphyrin molecule (figure 4.1), which in plants and cyanobacteria is reduced by the enzyme protochlorophyllide oxidoreductase (POR) to form chlorophyllide (Chl)ide, the last precursor in the biosynthesis of chlorophyll. The enzymatic catalysis has been studied *in vivo* and in etioplast membrane preparations⁽⁶⁾ and recently in reconstructed complexes *in vitro*^(5, 16). Conversion of Pchl)ide into Chl)ide occurs in several steps and involves both light-dependent and light-independent transformations^(5, 18, 19, 37, 38, 81). The reaction is triggered upon the absorption of light by Pchl)ide, and involves the transfer of two electrons and two protons, followed by the release of the products, Chl)ide and NADP⁺. When the POR:NADPH:Pchl)ide complex is illuminated at low temperature, the reaction can be trapped in an intermediate state and the intermediates can be characterized by fluorescence and absorption spectroscopy. By increasing the temperature one can force the reaction to proceed towards the next intermediate. Heyes and Hunter^(17-19, 38, 81) revealed, using this method, the presence of a number of intermediates in the dark stage of the reaction with different absorption and fluorescence properties. The absorption and fluorescence spectra of the reaction intermediates were found to gradually change between 696 nm and 671 nm, upon rearrangement of the active site of the protein, release of NADP⁺ and rebinding of the NADPH cofactor. Using this method in combination with EPR, ENDOR, and Stark spectroscopy, it was proposed that the first, non-fluorescent, intermediate with a broad absorbance band at 696 nm is a charge-transfer complex resulting from H⁻ (hydride) transfer from the NADPH molecule to the C17 position of Pchl)ide⁽³⁷⁾. This was supported by the observation of a NADPH/NADPD kinetic isotope effect⁽⁵⁵⁾ (KIE) on the rate of formation of the 696 nm intermediate, occurring with a time constant of 0.5 μ s. In the same study, a subsequent solvent KIE on the next step in the reaction with a time constant of 40 μ s was reported, and suggested to represent the proton transfer from the donor, a tyrosine residue, to the Pchl)ide molecule⁽⁵⁵⁾.

The initial ultrafast steps associated with the conversion of Pchl)ide into Chl)ide at room temperature, were studied with femtosecond transient absorption spectroscopy^(20, 52). In these experiments, the Pchl)ide molecule was excited at 475 nm by a 30-fs laser pulse, and the resulting absorption changes were detected in the 600-750 nm spectral range. It was shown^(20, 52) that upon ultrafast laser excitation an intermediate in the catalytic reaction is formed from the initially excited state, with effective rates of ~ 300 ns⁻¹ and ~ 3.7 ns⁻¹. The intermediate is an excited state emitting at 675 nm and is denoted as I675*. The I675* catalytic intermediate can only be formed after the enzyme has undergone a light-induced conformational change, triggered by a preceding photon absorption event, which most likely involves a structural reorganization of the active site⁽⁵²⁾.

The observed spectral changes upon illumination of Pchl_a reflect the catalytic conversion of Pchl_a into Chl_a, but may also reflect changes in the H-bonding environment and electrostatic interactions in the active site of the protein, prior and during the actual catalytic reaction, that affect the absorption and emission properties of the ground and electronically excited states of Pchl_a and Chl_a. For example, the binding of Pchl_a to the POR enzyme, which only occurs after binding of NADPH⁽⁶¹⁾, leads to a shift of 12 nm in the Pchl_a absorption, from 630 nm to 642 nm^(19, 61).

A better understanding of the catalytic reaction steps the pigment undergoes in the active site of the protein, and the role of the electrostatic and hydrogen bonding environment, can be obtained through studying the photochemical processes of Pchl_a in different solvents. Recently, the excited-state processes of Pchl_a in a variety of solvents (methanol, acetonitrile, cyclohexane) were studied using time-resolved fluorescence and pump-probe spectroscopy⁽⁸³⁻⁸⁶⁾. The experiments revealed Pchl_a to be an intrinsically reactive molecule, and the complex dynamics were interpreted with a model describing the excited-state processes in terms of a branching of the initially excited state population into a reactive and a non-reactive path, corresponding to populations of blue and red emissive states, respectively. The reactive path involved the formation of a state with intramolecular charge-transfer character in 27 ps and its subsequent decay in 200 ps. The non-reactive path displayed vibrational relaxation in 3.5 - 4 ps only, and was populated only in polar solvents. Based on time-dependent density functional theory calculations, a slightly different interpretation was proposed by Zhao and Han⁽⁴¹⁾, where the S₁ states of both the isolated Pchl_a, and its coordinated and hydrogen-bonded complexes, have an intramolecular charge-transfer character. As it was only the 4 ps process that was common to all solvents, they assigned this time constant to ultrafast vibrational relaxation and vibrational energy redistribution of the initially excited S₁ state with ICT (intramolecular charge-transfer) character. The process is followed, in polar solvents, by site-specific solvation in 27 ps, resulting in a strongly coordinated and hydrogen-bonded intermediate state.

Here, we report the results of time-resolved fluorescence, ultrafast visible and midinfrared pump-probe spectroscopic experiments of Pchl_a in several solvents (methanol, tetrahydrofuran, Tris/Triton water buffer solution) measured over a 3-ns time range upon excitation in the Soret region and upon direct excitation of the Q_Y band of the chromophore. Our data confirms the formation of a Pchl_a excited state with charge-transfer character, which in methanol is solvated via strengthening of the H-bonding interactions. The transient absorption data show a relatively intense and dynamic behavior of the excited state absorption spectrum. We demonstrate that the excited state lifetime of Pchl_a in all solvents lies in the range between 2 and 5 ns, and that the multi-exponential loss of signal in fluorescence and transient absorption experiments is due to a quenching of

the radiative rate only. We resolve the signature of the triplet state formed on a ns time scale, in the visible and IR regions. The vibrational frequencies of the C=O keto group on the cyclopentanone ring in Pchl_{ide} in the ground and electronically excited state are identified. Also, we present time-resolved transient absorption measurements of chlorophyll *a* (Chl *a*) in tetrahydrofuran to better illustrate that the excited state dynamics of Pchl_{ide} are intrinsically more dynamic than those of chlorophyll *a*.

5.2. Material and Methods

Sample preparation

Protochlorophyllide was extracted from *Rhodobacter capsulatus* ZY5 as described previously⁽³⁸⁾. Samples were dissolved in methanol (MeOH) or tetrahydrofuran (THF) (Sigma Aldrich), in D₂O (Merck) buffer (50 mM Tris pH 7.5, 100 mM NaCl, 1% Triton X100). Chlorophyll *a* from spinach was purchased from Sigma-Aldrich Chemie bv. The optical density of the Q_Y band of samples used for transient absorption measurements was between 0.2-0.4, for fluorescence measurements this was reduced to 0.05-0.1.

Steady-state spectroscopy

Steady-state visible absorption spectra were recorded using a Perkin Elmer Lambda 40UV/VIS spectrograph, steady-state fluorescence upon excitation at 400 nm, through a 1 nm wide slit, was collected with a Fluorolog FL-1039 apparatus.

Transients absorption (TA) spectroscopy

Visible transient absorption measurements were performed by exciting the red edge of the Soret transition of Pchl_{ide} at 475 nm or by excitation of the Q_Y band at 630 nm with a 50 fs laser pulse, and monitoring the resulting absorption changes in the Q_X and Q_Y electronic transitions of Pchl_{ide} by a 480-740 nm white-light probe beam. The probe beam was dispersed in a 2 nm resolution spectrograph (Chromex 250IS) and imaged on to a 256-element diode array. The instrument response function of the setup was about 120 fs, and the experiments were performed at a 1 kHz repetition rate; the setup has been described in more detail in Groot *et al*^(64, 67). Transient absorption mid-IR spectra were measured in the 1580-1780 cm⁻¹ region upon excitation at 400 nm, using the experimental setup as described in Groot *et al*^(64, 67). Typically, an excitation energy of 200 nJ focused onto a ~160 μm diameter spot size was used. In both TA experiments the pump beam was sent over a delay line, enabling the measurement of absorption difference spectra at time delays from -15 ps to 5 ns. In every experiment the relative polarization of the pump and probe light

were oriented at the magic angle (54.7°). One experiment resulted in a dataset consisting of TA signals recorded at 256 spectral channels and 50-60 positions of the delay line, where one dataset is an average of 30-50 single scans over the delay line, with 250 laser pulses acquired at each delay position. Measurements for each solvent were repeated 2-3 times in different experimental sessions. A 200 μm path cell was used for the samples, which was mounted into a Lissajous sample scanner to collect the signal from a fresh sample spot for each subsequent laser shot.

Time-resolved fluorescence

Time-resolved fluorescence was collected in the 450-750 nm spectral region, using a synchroscan streak camera Hamamatsu C5680, upon 400 nm excitation with a 50 fs laser pulse, at a 250 kHz repetition rate on time bases of 250 ps, 500 ps, and 2.2 ns. The setup has been described in more detail in van Stokkum *et al.*⁽⁸⁷⁾. The instrument response function of the setup was adequately modeled by a Gaussian shape with parameters μ and Δ for, respectively, location and full width at half maximum (FWHM). FWHM in our measurements was estimated as 3.5-4.5 ps in the 200 ps time window, 5.8-6.7 ps in the 500 ps window, and 20 ps in the 2200 ps time window. For the time-resolved fluorescence measurements the sample was in a stirred 1 cm quartz cell.

Data analysis

All data were fitted with a global analysis procedure in which all wavelengths are fitted simultaneously by a sum of exponentials, either applying a sequential or a parallel kinetic scheme⁽⁸⁸⁾. The dispersion of the probe light was fitted as a second order polynomial. Data is presented in the form of evolution-associated difference spectra (EADS), resulting from a sequential scheme. The fluorescence decay is presented in the form of evolution-associated spectra (EAS).

5.3. Results

5.3.1. Absorption and fluorescence steady-state spectra

Figures 5.1.A, B show the absorption and fluorescence spectra of Pchl_a recorded in tetrahydrofuran (THF) and methanol (MeOH). Both absorption and emission spectra have been normalized to the amplitude of the signal of the Q_Y band. In the polar aprotic THF solvent, Pchl_a has a narrow Q_Y absorption band, peaking at 628 nm. In the polar H-bonding solvent methanol, both the Soret region and the red shoulder of the Q_Y band

experience broadening, and the peak of the Q_Y band shifts to 629.5 nm. Pchlide dissolved in buffer, either in H_2O or D_2O , produces spectra very similar to methanol (not shown). The 577 nm and 580 nm bands, in methanol and THF respectively, can be ascribed to the energetically higher lying Q_X absorption bands.

The fluorescence emission spectra recorded upon 400 nm excitation in THF and methanol are shown in figure 5.1.B. The emission from the principal $(1-0)\leftrightarrow(0-0)$ transition appears at 630-631 nm in both cases, and thus shows a very small Stokes shift. The less intense band at 682 nm is likely to represent the vibronic $(1-0)\leftrightarrow(0-1)$ transition. In methanol, the emission spectrum is significantly broader than in THF, and the band at 682 nm is much more intense. There is also a minor feature at 596 nm in THF, and a broader band at 585 nm in methanol, which could be due to emission from the Q_X transitions.

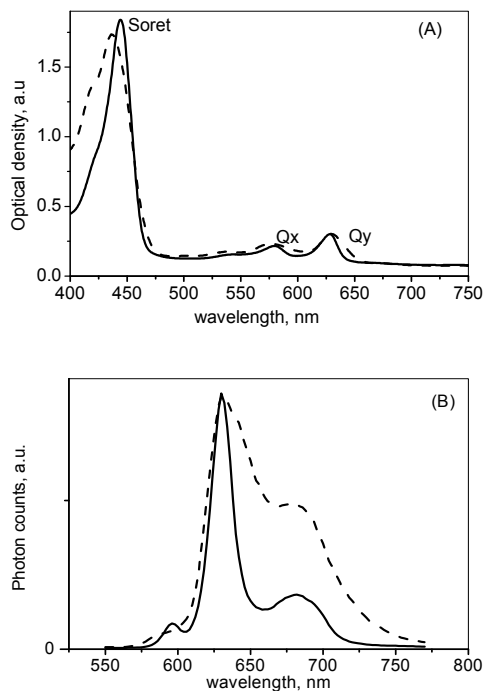


Figure 5.1 (A) Visible absorption spectra of Pchlide in THF (solid) and MeOH (dashed). (B) Corresponding fluorescence emission spectra of Pchlide in THF (solid) and MeOH (dashed) recorded at 400 nm excitation.

5.3.2. Time-Resolved Fluorescence

The fluorescence decay dynamics of Pchl_a measured in THF, methanol and H₂O/Tris/Triton buffer upon excitation at 400 nm are shown in figure 5.2. The datasets were recorded in three time ranges of 250 ps, 500 and 2200 ps, and then analyzed simultaneously using a sequential decaying scheme with either three or four components, in which $A \rightarrow B \rightarrow C \rightarrow D \rightarrow^{21}$.

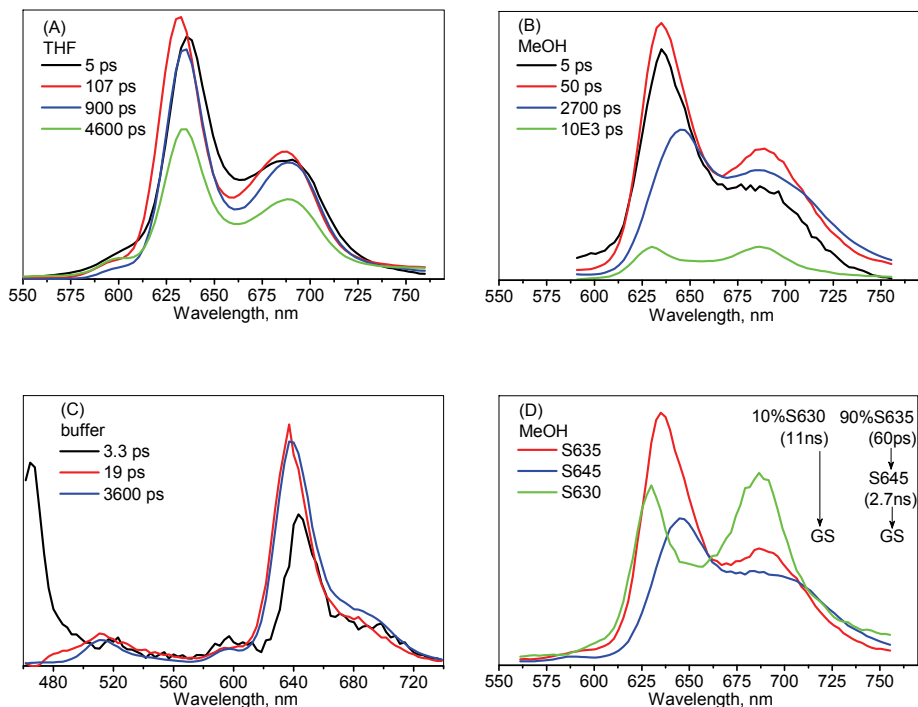


Figure 5.2. EAS of time-resolved fluorescence of Pchl_a upon 400 nm excitation in different solvents obtained by global analysis using a sequential decaying scheme: **(A)** THF; **(B)** MeOH; **(C)** buffer; **(D)** Species-associated spectra of Pchl_a in MeOH in 2.2 ns time window obtained in fitting the data with branched kinetic scheme. Note that the initial red spectrum corresponds to the red spectrum in panel B.

In THF, the data were fitted globally with four exponential lifetimes of 5 ps, 107 ps, 900 ps and 4.6 ns (figure 5.2.A). As in the steady-state regime, the emission of Pchl_a arises from a main electronic transition $(1-0) \rightarrow (0-0)$ and from a vibronic $(1-0) \rightarrow (0-1)$

transition, separated from the main band by $\sim 1300\text{ cm}^{-1}$. In THF initially, at $t = 0$ ps delay after excitation, the spectrum peaks at 635-636 nm. The emission blue-shifts to 631 nm and increases in intensity with a time constant of 5 ps, followed by a small decay and red-shift of the spectrum back to 634 nm after 107 ps. In 900 ps half of the emission decays, with the remainder having a lifetime of 4.6 ns and peak positions at 634 and 688 nm. The initial gain and blue-shift of the emission are absent in the Pchlide spectra in THF upon direct excitation of the blue shoulder of the Q_Y band at 620 nm (data not shown).

The data in methanol from all time windows was best fitted simultaneously with a common set of lifetimes of 5 ps, 50 ps, 2700 ps and 10 ns. The initial spectrum peaks at 635 nm and evolves after 5 ps into a more intense spectrum peaking also at 635 nm, similar to the initial dynamics in THF. After 50 ps, this is followed by a decrease of emission and a significant red-shift of the principal band to 645 nm, accompanied by a broadening of the vibrational band at 688 nm. This spectrum (blue line) has a lifetime of about 2700 ps, after which a weak emission remains (green line), characterized by two bands of equal intensity, peaking at 630 nm, and at 686-687 nm (energy difference of 1300 cm^{-1}). This spectrum has a lifetime of about 10 ns.

To test for the possibility that a species characterized by the 10-ns spectrum is already present at $t=0$ ps, we fitted the data to the scheme as depicted in figure 5.2.D, ignoring the initial 5-ps dynamics. Here, the main emission arises from a state which we denote S1. This is characterized by a maximum at 635 nm, which evolves in 60 ps to a state denoted as S645 with a lifetime of 2700 ps. In parallel, there is a minor emission from a state denoted as S630/686, which shows no evolution and has a lifetime of 10 ns. The species-associated spectra that result from this analysis are shown in figure 5.2.D. The amount of S630/686 estimated in this way is only 10%. This analysis resulted in a fit quality that was as good as that of the sequentially decaying scheme.

The data obtained with Pchlide dissolved in Tris/Triton buffer solution was collected in a wider spectral region than for the THF and methanol experiments. The data could be globally fitted with three exponentials with lifetimes of 3.3 ps, 19 ps, and 3600 ps. Similar to methanol and THF, the initial evolution (black to red evolution in figure 5.2.C) is accompanied by a significant gain in the intensity at the blue side of the Q_Y band, resulting in a blue-shift of the emission maximum from 643 nm to 637 nm after 3.3 ps. But in this case, due to the extended spectral window, we can clearly observe an additional band at 465 nm in the black spectrum, which disappears simultaneously with the gain in the Q_Y region. Therefore, this band is most likely due to emission from the S2 electronic state of Pchlide, implying that relaxation from the S2 to S1 state is not complete on the 3 ps timescale. Very minor spectral evolution occurs after 19 ps resulting in a small gain on the red side of the

(1-0)→(0-0) band and (1-0)→(0-1) band. In addition, a weak emission shoulder around 590-600 nm is resolved in all solvents.

5.3.3. Visible Transient Absorption Spectroscopy

The results of the visible transient absorption measurements in the 500-740 nm spectral region are shown in figure 5.3, in the form of evolution-associated difference spectra (EADS), resulting from applying a sequential model ($A \rightarrow B \rightarrow C \rightarrow D \rightarrow$) to the data. Negative bands in the EADS represent a bleach of the ground state absorption or stimulated emission (SE); positive signals correspond to absorption from the excited state to higher lying levels (ESA).

The transient absorption dynamics of Pchl_{id} in THF both upon 475-nm and 630-nm excitation is best fitted with a set of four time constants of 0.7 ps, 9-10 ps, ~900 ps, and 3400 ps. When excited in the Soret, after 0.7 ps an increase in the SE and blue-shift from 633 nm to 631 nm of the absorption difference spectra occurs (figure 5.3.A). Remarkably, in the initial EADS, stimulated emission from the Q_X band is resolved, in agreement with the decay of signal around 600 nm in the fluorescence emission experiment. After 10 ps, a minor further increase of the signal occurs with an additional blue-shift to 629 nm, followed by decay with time constants of 900 ps and 3400 ps. When the low-energy Q_Y transition in Pchl_{id} is directly excited at 630 nm (figure 5.3.B), the initial increase and blue-shift of the stimulated emission are completely absent. Instead, a multi-exponential decay of the signal is observed. Time traces of transient absorptions collected at 630 nm from both experiments are shown in figure 5.4. They clearly demonstrate a remarkable difference in the initial 10-100 ps phase, but a similar time-dependence thereafter.

We included an additional fifth component into our sequential global model ($A \rightarrow B \rightarrow C \rightarrow D \rightarrow E \rightarrow$) in order to test whether the spectrum of a long-lived bleaching of the ground state absorption due to population of a triplet state could be resolved. To this end we deliberately fixed the lifetime of the fifth component to 1.5 ms. As a result, a set of five time constants was obtained of 0.7, 10, 900 ps, 2.4 ns and 1.5 ms. The final 1.5 ms EADS has a distinctly blue-shifted spectral shape, with a bleach at 625 nm, and less intense ESA. We can obtain an estimate for the quantum yield of triplet formation by calculation of the ratio of integrals between the first $t=0$ ps EADS and the fifth EADS. For Pchl_{id} in THF, excited at 630 nm, we obtain in this way $\Phi_T \sim 12\%$, although when we correct for a maximal contribution of 50% of SE in the $t=0$ ps negative signal, then the estimate is $\sim 23\%$.

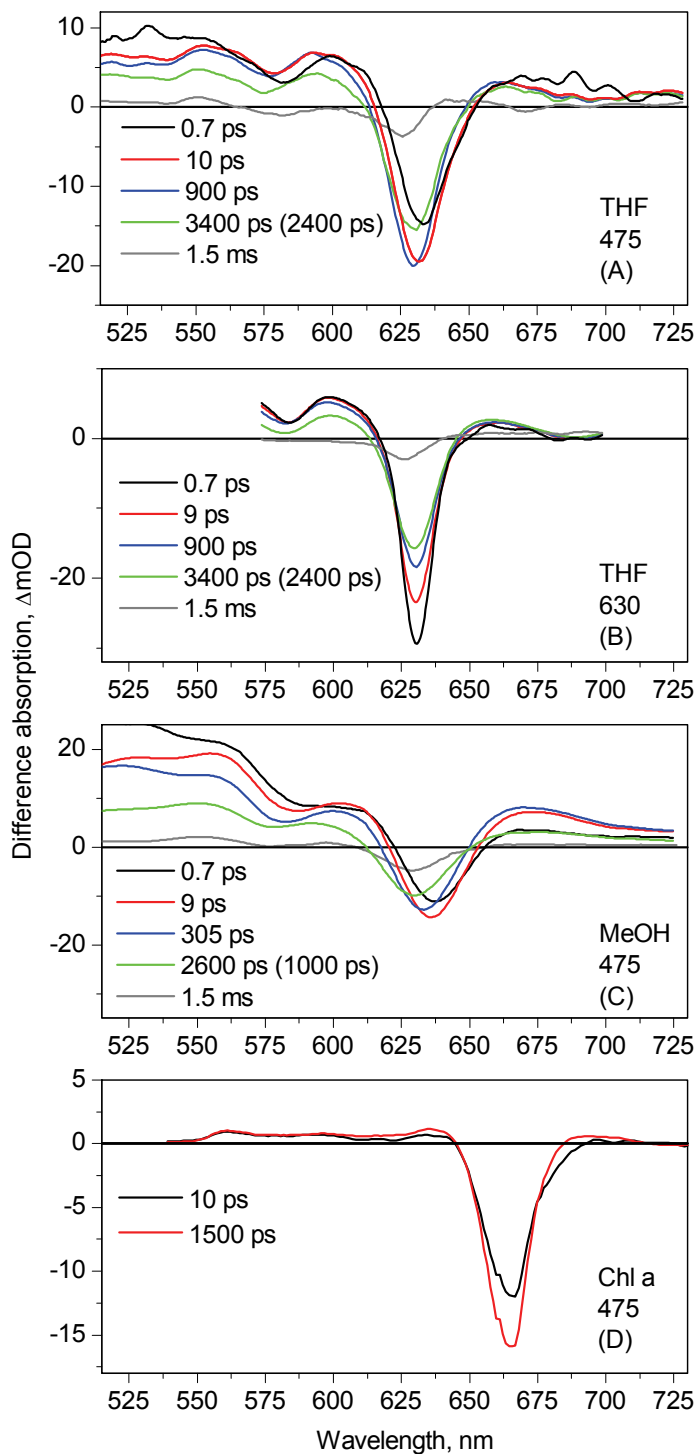
Pchl_{id} in methanol excited at 475 nm (figure 5.3.C) also shows an increase of blue emission in 0.7 ps, followed by a multi-exponential blue-shift of the negative signal from 639 nm to 636 nm, which is likely to originate from a decay of the red SE, and

accompanying changes in the ESA. These dynamics are best described by exponentials with lifetimes of 9 ps, and 305 ps and 2.6 ns. For this dataset we applied the same procedures as for THF, to extract a long-lived spectrum for the transition to a triplet state. As a result, the long-lived dynamics could be split into 1 ns and 1.5 ms. After 1 ns, part of the bleaching and the SE decays, and a bleached absorption signal remains. This state has a blue-shifted spectrum, as in THF, but peaks at 629 nm. The Pchl_{ide} in methanol TA spectra show a more intense ESA continuum band than those of Pchl_{ide} in THF. In addition, in methanol the ESA in the 650-725 nm spectral region shows a significant gain after 0.7 and 9 ps, whereas in the 500-620 nm region the ESA decays. In THF, this effect is not present to such a degree. We further note that the spectral shifts of the Q_X bleach, superimposed upon the ESA, follow the same dynamics as those in the Q_Y region.

The analysis of the TA and fluorescence data yielded slightly different time constants (see table 5.1). We tested whether it was possible to obtain a simultaneous fit of the TA and fluorescence data, for both THF and methanol, linking the corresponding EAS and EADS to get a unified set of lifetimes. Using four components ($A \rightarrow B \rightarrow C \rightarrow D \rightarrow$) this resulted in minor but noticeable misfits in the TA data. Increasing the number of components ($A \rightarrow B \rightarrow C \rightarrow D \rightarrow E \rightarrow$) in the simultaneous fit resulted, however, in some of the components having no associated spectral change in fluorescence spectra. We conclude therefore that the difference in the obtained lifetimes is real, and describes a dynamic difference between the TA and fluorescence data.

Transient absorption measurements on chlorophyll *a* (Chl *a*) in THF in the Q_Y region were performed using 475-nm excitation (figure 5.3.D). The data were best fitted by only two exponential decaying components with lifetimes of 10 ps and 1500 ps. Also, this data shows an increase of negative signal in the first evolution. A comparison of the traces recorded at 665 nm of Chl *a* excited at 475 nm, with those of Pchl_{ide}, clearly shows the same effect of initial emission increase, as was observed for Pchl_{ide} for the first 10 ps. However, the following decay of SE and GS bleach recovery occurs faster in Chl *a* than in Pchl_{ide}. Also, the ESA in Chl *a* seems to be much weaker than is observed in Pchl_{ide}. Therefore, Pchl_{ide} demonstrates more complicated excited state decay dynamics compared to Chl *a*.

Figure 5.3. EADS of transient absorptions of (A) Pchl_{ide} in THF excited at 475 nm (B) Pchl_{ide} in THF excited at 630 nm (C) Pchl_{ide} in MeOH excited at 475 nm (D) Chl *a* in THF excited at 475 nm. The lifetime in brackets for the fourth spectrum in panels A, B, C is obtained when the triplet state (fifth spectrum) was included in the global analysis.



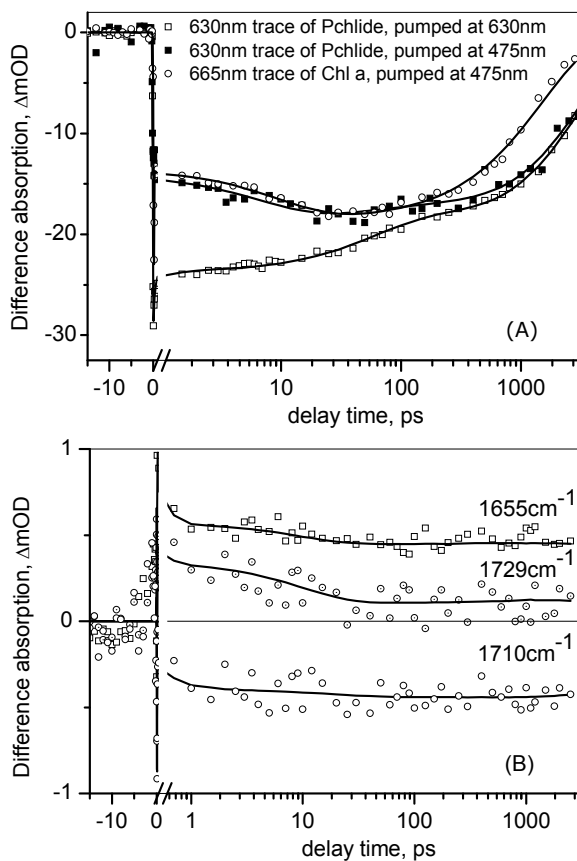


Figure 5.4. (A) The 630 nm traces of transient absorptions and fit of Pchl_{ide} in THF excited at 630 nm (red line and open squares), excited at 475 nm (blue line filled squares), and the 660 nm trace of Chl a excited at 475 nm (black line open circles). (B) The mid-IR transient absorptions traces of Pchl_{ide} in THF, excited at 400 nm. The associated lifetimes are shown in table 5.1. The lifetime of the long-lived state for the mid-IR measurement was estimated to be more than the available delay line of 3 ns, therefore is referred as infinite

A short summary of our observations in the visible part of the spectrum is: (i) the initial blue-shift and increase of emission in the Q_Y region is present only upon S₂ excitation and is due to S₂ to S₁ internal conversion, probably occurring in conjunction with vibrational cooling; (ii) quenching of the S₁ emission is a multi-exponential, with an evident shortening of the S₁ excited state lifetime in methanol, probably reflecting higher

reactivity due to the H-donating properties of methanol; (iii) the S1 excited state dynamics of Pchl_a are more complicated than that of Chl *a*.

5.3.4. Mid-IR Transient Absorption Spectroscopy

To investigate the excited state dynamics via the responses of the C13¹=O keto and C13²=O ester modes of Pchl_a, and to determine the role of H-bonding on the excited state dynamics, we recorded transient absorption spectra of Pchl_a in different solvents in the spectral region between 1780 and 1580 cm⁻¹ upon excitation at 400 or 475 nm. These groups are the most intense IR markers in the selected region, since they are closely located to the conjugated electronic macrocycle. The C17 carbonyl group located much further therefore their contribution to the difference absorption signal upon electronic excitation is negligible. Also the C17 bands are likely to be much higher in frequencies compared to the C13 keto vibrations.

The EADS resulting from fitting the dynamics of Pchl_a in THF, methanol, D₂O buffer solution are shown in figure 5.5. Negative bands in these spectra belong to the bleached absorption of the vibrational transitions in the ground state and positive bands represent the absorption due to the vibrational transitions of the Pchl_a molecule in the electronically excited state. The data in THF, methanol and D₂O buffer were well fitted using a sequential scheme with only two exponentials (A→B→).

The mid-IR difference spectra of Pchl_a in THF (figure 5.5.A) have a negative band at 1708 cm⁻¹, typical for a non-hydrogen-bonded 13¹-keto band^(45, 71, 89-91). In the excited state the keto mode downshifts to ~1658-1665 cm⁻¹, and shows a small upshift after 7 ps. The structure superimposed on the spectrum in this region is most likely due to the absorption changes of less intense modes of the macrocycle skeleton. In the ester region above 1725 cm⁻¹, there is initially a band shift structure with a negative band at 1750 cm⁻¹ and a positive band at 1730 cm⁻¹, which after 7 ps develops into a structure with reduced amplitude of a negative signal at 1750 cm⁻¹ and positive peak at 1738 cm⁻¹. In chlorophyll and pheophytin, the ester mode downshifts in the excited state from 1740-1750 cm⁻¹ to 1724-1732 cm⁻¹ in non H-bonding solvents. For example, the ester mode of Chl *a* in THF in the ground state was found at 1740 cm⁻¹ and the keto around 1698-86 cm⁻¹, but in the excited state the ester band downshifts to 1726 cm⁻¹ and the keto appears at 1650-1640 cm⁻¹ (92).

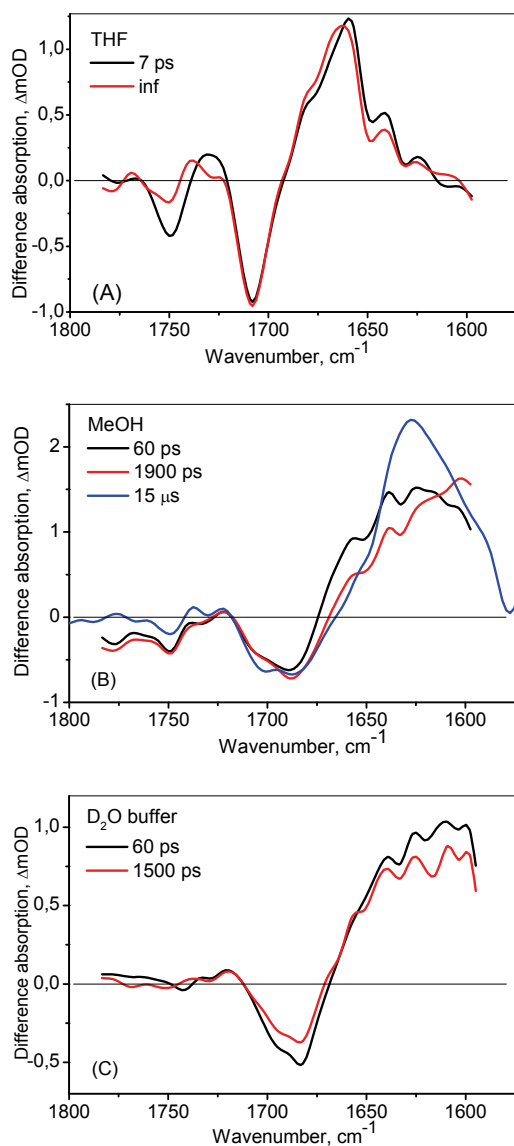


Figure 5.5. EADS resulting from global analysis of (A) Pchlide in THF excited at 400 nm; (B) Pchlide in methanol excited at 400 nm, blue line – the FTIR spectrum in methanol recorded after 15 μs after excitation with a 5 ns 444 nm laser pulse; (C) Pchlide in D₂O Tris/Triton buffer excited at 475 nm.

Pchl_a in the polar solvent methanol has multiple negative bands (figure 5.5.B). The spectrum at $t = 0$ ps shows two bands in the keto region, at 1705-1701 cm^{-1} , slightly lower than for the C13 keto in THF, and at 1687 cm^{-1} . The presence of two keto frequencies in the ground state is a clear indication of two groups of Pchl_a populations, with different strength of either H-bonding or coordination interaction. The negative band due to the ester mode is at 1750 cm^{-1} , which downshifts in the excited state to 1740 cm^{-1} and 1722 cm^{-1} . The very broad positive structure at 1625 cm^{-1} is again due to keto modes in the excited state. A further downshift of the excited state feature around 1625 cm^{-1} occurs in 60 ps (black to red evolution). It should be noted that in the visible region, this corresponds to the decay and red shift in the emission from 635 to 645 nm.

The result of a step-scan FTIR measurement on a metastable Pchl_a state, presumably a triplet state, that lives about 15 μs , is superimposed on the result of the TA experiment (blue spectrum in figure 5.5.B). This spectrum has a better resolved high frequency band at 1700 cm^{-1} , and a low frequency mode at 1686 cm^{-1} . The shortened lifetime of the triplet as compared to the 1.5 ms lifetime of the Chl *a* triplet⁽⁹³⁾, is most likely due to quenching of the triplet state by oxygen, since the methanol solution was not deoxygenated before the measurement. The positions of the negative keto and ester peaks coincide with those in the ultrafast measurement.

The positive 1625 cm^{-1} band in methanol is fairly low in frequency as compared to the band at 1660 cm^{-1} in THF. The bacteriopheophytin anion/neutral difference spectrum⁽⁴⁵⁾ has bands at 1658-1627 cm^{-1} , and around 1580 cm^{-1} . The carbonyl frequencies of the bacteriochlorophyll anion⁽⁹⁴⁾ were observed around 1643, 1620 and 1592 cm^{-1} . Therefore, the downshift of the keto band after 60 ps could be indicative of anion formation. On the other hand, the low-frequency position of the keto mode in the excited state can be the result of the H-bonding in Methanol, and the further downshift in 60 ps to increased H-bonding due to solvation. This will be discussed in more detail in the Discussion section.

Pchl_a in buffered D₂O solution (figure 5.5.C) shows an initial spectrum with double-peaked negative bands at 1695 and 1683 cm^{-1} , which develops in 60 ps into a similar spectrum with slightly decreased amplitude of the negative bands and a slightly decreased broad positive band below 1670 cm^{-1} . The signal of the ester band is found at 1742 cm^{-1} . The fact that both keto bands are located at lower frequency than the 1708 cm^{-1} mode in THF implies that both keto groups experience some degree of H-bonding with the solvent.

In table 5.1 we have collected the lifetimes in picoseconds as obtained from the global analysis of the dynamics of Pchl_a in various solvents, by visible and mid-IR

transient absorption spectroscopy and by time-resolved fluorescence emission measurements.

Table 5.1. Time constants in picoseconds (if not mentioned otherwise) for Pchl_{ide} excited state dynamics obtained from the global fit of the data in several solvents measured with different techniques.

solvent	method	T1	T2	T3	T4	T5
THF	Fluorescence	5	107	900	4600	-
	Vis TA	0.7	10	900	3400	1.5 ms
	mid-IR TA	7	-	-	inf	-
Methanol	Fluorescence	5	50	-	2600	-
	Vis TA	0.7	10	300	2600	1.5 ms
	mid-IR TA	-	60	-	1900	-
	FTIR	-	-	-	-	15 μ s
Water buffer	Fluorescence	3	19	3660	-	-
	mid-IR TA	-	60	1500	-	-

5.4. Discussion

The experiments performed in the visible and in the mid-IR spectral regions show that the excited state dynamics of Pchl_{ide} are complex, strongly influenced by the solvent, and are also dependent on the wavelength of excitation. In the following section we will discuss these dynamics and the mechanisms of the excited state decay in more detail.

5.4.1. Dynamics of Pchl_{ide} in THF upon 630 nm excitation

The dynamics of Pchl_{ide} in THF without major interference from electronic and vibrational relaxation processes can be inferred from the 630-nm excited TA dataset (figure 5.3.B). The data display a multi-exponential decay of signal, accompanied by only a very minor blue-shift, occurring on the 0.7 ps, 10 ps and 900 ps timescale, amounting to about 50% (see also the fluorescence Streak data in figure 5.2.A), after which the excited state decays on the 3.4 ns time scale. The decay of the excited state is partially into a metastable triplet state, whose absorption difference spectrum is clearly different from the singlet excited state difference spectra, due to the stimulated emission and strong excited state absorption in the latter. The mid-IR difference spectra demonstrate very little dynamics (within the obtained signal to noise ratio) over a few ns time scales (see figure 5.4.B), showing that the

decay in the fluorescence and transient absorption experiments is a quenching of the radiative rate, rather than a population decay of the excited state.

Chlorophyll-like molecules in solution have a coordination state⁽⁹⁵⁾ of the central magnesium atom of 5 or 6. Different coordination interactions of chlorophyll with the solvent molecules and between two chlorophylls are possible, involving the central magnesium ion and the polar C=O groups. THF is an aprotic and electron-rich (1.63 D) solvent that is moderately polar with a dielectric constant of 7.6, which can act as a strongly coordinating ligand. For Pchl_a it has been demonstrated⁽⁹⁵⁾ that THF results in the monomer state with all pigments having identical electrostatic environments. Hence, it is highly unlikely then that the π electronic clouds of adjacent molecules overlap with each other, resulting in the narrow, blue-shifted and symmetrical, Q_Y band at 628 nm. In THF, there is only one population of the C13 keto mode in the mid-IR TA spectra, confirming that there is *no* coordination interaction between Pchl_a molecules, involving the keto group. If this was the case, at least two populations would have been found, similar to Pchl_a in methanol.

Therefore, the quenching of the radiative decay is most likely due to the solvation of the internal charge-transfer state in Pchl_a by the coordinating THF ligand, and THF solvation shell. Time-dependent density functional calculations⁽⁴¹⁾ indicated that the S1 states of both the isolated and solvated Pchl_a have an intramolecular charge-transfer character. In addition, in protic solvents, site-specific solvation should result in strengthening of the H-bonding pattern, and an even stronger charge-transfer character, leading to the formation of a 'dark' state, with reduced oscillator strength⁽⁴¹⁾. We conclude that in THF, the polarity of the solvent results in a multi-exponential solvation of the ICT state, which can be described with time constants of 0.7 ps, 10 ps and 900 ps. The final state, with a 3-4 ns lifetime, has a reduced but still significant oscillator strength, as judged from the presence of fluorescence emission on the ns timescale. From this state, a triplet state is formed with a yield of ~23%.

5.4.2. Dynamics of Pchl_a in THF upon 475 nm excitation

The same solvation of the ICT state undoubtedly occurs upon excitation at 475 nm, but prior or in parallel to that, the excited state partly relaxes to the S1 state. The observed dynamics show that this internal conversion is unexpectedly slow and apparently extends to the 0.7 ps time scale. Possibly, this is related to the ICT character of the S1/Q_Y state, which may slow down the internal conversion process between the two states.

An initial increase and blue-shift of the stimulated emission is observed with time constants of 0.7 ps in Pchl_a in THF and methanol, when excitation in the Soret region is

used. Upon direct excitation of the Q_Y transition these initial dynamics are absent. Also in the measurements of the time-resolved fluorescence upon red excitation (620 nm) the blue species did not appear (data not shown). Remarkably, the pump-probe spectra show stimulated emission from the Q_X transition on the same timescale, and the fluorescence Streak camera images show, for the wide spectral range experiment on Pchl_{ide} in buffer, emission from the Soret within the IRF. We conclude therefore, that the S₂ to S₁ internal conversion is multiphasic, and that although a part of the excitations relax via the Q_X to the Q_Y transition within the instrument response function (IRF) of the visible pump-probe experiment (i.e. faster than 120 fs), a significant fraction relaxes only in ~ 700 fs. Also, it is likely that corresponding dynamic changes in the ESA contribute to the net blue-shift of the negative transient absorption signal. The 3-5 ps process resolved in the Streak fluorescence emission experiment probably partly represents the same process, but is limited by the IRF of the Streak camera. A gain of emission for Pchl_{ide} dissolved in methanol occurring within the 3.5 ps IRF of a streak camera has been reported earlier⁽⁸⁴⁾, upon excitation in the Soret. Here, we show that this effect is a consequence of exciting with excess energy in the Soret transition.

The slower spectral evolution of 10 ps resolved in the TA data of chlorophyll, the 9-10 ps process in the visible dynamics of Pchl_{ide} in THF and methanol, and partially the 3-5 ps process in the emission data, also show an increase in blue emission that is probably due to vibrational relaxation. The Q_Y transition is populated with excess thermal energy, and the funneling of this energy into a specific mode may lead to a blue-shift of the emission spectrum while cooling, when the overlap of the wavefunction with wavefunctions high on the ground state energy surface is different. The dynamics in the mid-IR spectra of Pchl_{ide} in THF, showing a 7-ps upshift of the ester band from 1730 to 1738 cm^{-1} (figure 5.5.A and C), is consistent with vibrational energy relaxation. An upshift of the C=O keto mode of about 7 cm^{-1} in the excited state, due to intramolecular vibrational redistribution and vibrational cooling, has been observed in several other aromatic molecules⁽⁹⁶⁻⁹⁸⁾. The lower signal-to-noise level and the more complicated mid-IR spectra have probably prevented this observation for Pchl_{ide} in methanol. For Chl a, vibrational energy relaxation processes have been assigned to dynamics in the visible part of the spectrum occurring on the sub-ps^(99, 100) to a few picoseconds timescale⁽¹⁰¹⁾, and are usually not separated from dielectric relaxation processes. A similar red-shifted stimulated emission followed by a blue-shift on the 10 ps timescale has been reported for porphyrin molecules that had been excited with excess vibrational energy⁽¹⁰²⁾. Rodriguez *et al*⁽¹⁰²⁾ attribute the red-shifted emission to a decrease in the energy gap between electronic states, as a consequence of a decrease in the resonance integral. The resonance integral is decreased by the molecular expansion of the molecule due to the increase in temperature of the vibrationally hot porphyrin. With the

dissipation of the excess vibrational energy on the 10 ps time scale, the “normal” blue-shifted emission is restored. Hence, we conclude that upon Soret excitation of Pchl_{id}e and Chl_a, vibrational energy relaxation, possibly in conjunction with solvation, occurs with a slower 10 ps time constant. We note that in early measurements on chlorophyll *a* in pyridine⁽¹⁰³⁾ a similar effect of SE gain was observed between 10 ps and 300 ps after photoexcitation with a 7 ps excitation laser pulse at 355 nm. To our knowledge, later experiments in the literature on chlorophyll molecules, always used either excitation in the Q_Y or Q_X band, or a very narrow time window to monitor the ensuing ultrafast processes^(99-101, 104-106).

A further difference is that although the dynamics occur on the same timescales when Soret or Q_Y excitation is used, the extensive quenching of the signal (i.e. of the stimulated emission) is much less important when Soret excitation is used, whereas the ESA in the 620-630 nm region seems to be more dynamic. This indicates that during the internal conversion from the S₂ to the Q_X and to the Q_Y states, the ICT state is solvated in a way that is more efficient (i.e. faster) than the corresponding process in the Q_Y state. Therefore, upon 475-nm excitation, it is not the fully emissive S₁ state that is populated but the solvated S₁/ICT state.

5.4.3. Dynamics of Pchl_{id}e in methanol upon 475 nm excitation

In methanol the dynamics are more complicated as the loss of fluorescence is accompanied by a relatively larger loss of emission from the (1-0)→(0-0) transition than emission from the vibronic (1-0)→(0-1) transition. In fact, the complex dynamics on the 60 ps and 2.7 ns time scale (red-shift of the emission, followed by a blue-shift resulting in a final 10-ns living spectrum with two peaks of equal amplitude at 630 nm and 686 nm) suggest a heterogeneity in the kinetics. Therefore, we applied a target analysis, allowing for a splitting of the reaction dynamics at *t*=0 ps and resolved the spectra of three states, one with a double-peaked spectrum termed S_{630/686} and another two with a more ‘classical’ spectrum, the first peaking at 635 nm, which after 60 ps relaxes into a state with an emission maximum at 645 nm (S₆₄₅) (figure 5.2.D). Note, that the S_{630/686} species is only a minor fraction of 10%.

Heterogeneity in the GS may originate from a difference in the structure of Pchl_{id}e itself, because two forms of native pigment are present in the sample preparation, namely divinyl Pchl_{id}e (DV-Pchl_{id}e) and monovinyl Pchl_{id}e (MV-Pchl_{id}e) in a 5:1 ratio. The steady-state absorption and emission spectra recorded at 77 K of the two forms are different in the Soret region⁽¹⁷⁾. The DV form has the maximum of the Soret band at 445 nm, whereas the MV form has its maximum at 439 nm. It is likely that this spectral shift arises

from the different degree of conjugation in the vinyl residue of Pchlride at the C8 position. In the Q_Y region at room temperature the DV form of Pchlride has its absorption maximum at 632 nm and the MV form at 629 nm^(107, 108). Taking into account that with excitation at 475 nm we would preferentially excite the DV form, it could very well be that our 10% S630/686 species can be identified as MV Pchlride. This form apparently has an unusually long excited state lifetime, and a remarkable double-peaked emission spectrum. We note that in the reaction with the POR protein the MV or DV forms of Pchlride show the same catalytic reaction and product yield⁽¹⁷⁾.

The main evolution in the emission, a 10 nm red-shift from 635 nm to 645 nm and a decay of about 50%, occurring in 60 ps, suggests that the excited state potential shifts, leading to a different overlap of the ES wave functions with those on the GS potential energy surface. This results in reduced fluorescence intensity and a modified emission spectrum, in agreement with the observations in THF, due to the solvation of the S1/ICT state.

Methanol is an H-bonding polar (1.69 D) solvent that provides five-coordinated interaction with chlorophyll molecules⁽¹⁰⁹⁾. The steady-state absorption spectrum of Pchlride in methanol is broader on the red side of the Q_Y band as compared to the Q_Y band in THF, and shifted by 1-2 nm to the red (figure 5.1.A). TDDFT calculations⁽⁴¹⁾ showed that the red-shift of the absorption and emission band is caused by H-bonding between Pchlride and methanol molecules. In fully optimized structures⁽⁴¹⁾ one coordinating interaction between the central magnesium and a methanol molecule was considered, and five additional site-specific H-bonded interactions provided by four methanol molecules per Pchlride. Moreover, it was shown that the coordination interaction between Mg and methanol causes a lowering of the S1 excited state absorption from 615 nm for isolated Pchlride to 631 nm, and further to 647 nm with additional H-bonding to the C=O residue at the C13 and C17 positions of the macrocycle. One more H-bonding interaction to the C=O keto at the C13 position was shown to cause further lowering of the excited state from 647 nm to 667-668 nm.

Our mid-IR TA experiment clearly demonstrates the presence of two groups of C13 keto ground state vibrations at 1700 cm^{-1} and 1686 cm^{-1} , which implies that there are two site-specific solvation patterns of the keto group in Pchlride in methanol with different strengths of interaction, either H-bonding to bulk solvent or a coordination interaction. The frequency of the 1700 cm^{-1} population is only moderately downshifted in comparison to the single and non H-bonding keto mode in THF at 1708 cm^{-1} , and may reflect the different polarity of methanol versus THF, rather than the presence of a (weak) hydrogen bond in methanol.

In the mid-IR data, we observe that the keto modes in the excited state are significantly lower in frequency than in THF. In addition, on the 50-60 ps time scale of the reduction of the radiative rate (loss of fluorescence intensity), the keto mode downshifts in frequency in methanol, but not in THF. This downshift can be interpreted as a strengthening of the hydrogen bonds between methanol molecules and the keto group of Pchl_{id}e. A similar H-bond strengthening in the excited state was described for fluorenone chromophores in methanol⁽¹¹⁰⁾, where the C=O stretching frequency in the electronically excited state downshifts about 160 cm⁻¹, the stretching frequency of the C=O group in the dye Coumarin 102 can downshift about 75 cm⁻¹ in the excited state in hydrogen bonding solvents as well⁽¹¹¹⁾, and electron transfer from the alcoholic solvent to the chromophore oxazine 750 was shown theoretically and experimentally to occur on an ultrafast timescale via site-specific solvent-solute hydrogen bonding facilitated by their strengthening^(110, 112). Indeed, for Pchl_{id}e in methanol, Zhao and Han⁽⁴¹⁾ proposed that, in the electronically excited state, a strengthening of the intermolecular H-bonding pattern takes place, including the keto C=O---HO hydrogen bond. It was also proposed that electron redistribution from the macrocycle to the C=O group upon ICT state formation may occur as well. Hence, the appearance of additional charge around the keto group, and/or dynamics in the H-bond on the keto group, should lead to a lowering of the dipole moment of the keto. However, we do not observe this effect in THF or in methanol.

We conclude therefore, that the ICT character of the Pchl_{id}e S1 excited state leads to a dynamic solvation of this state, causing a reduction of the oscillator strength. The hydrogen bond capabilities of the methanol solvent lead to a more extensive and faster solvation process, with the major fluorescence quenching occurring over a 50-300 ps time scale as compared to the 900 ps process in THF. The emission decay occurs in conjunction with a strengthening of the hydrogen bonds with the keto group of Pchl_{id}e. The S1 excited state lifetime in methanol is shorter than in THF (2.6 ns vs 3.4 ns). Indeed, a shortening of the Pchl_{id}e fluorescence lifetime in methanol has previously been demonstrated also by Mylsiwa-Kurdziel *et al*⁽¹¹³⁾.

For Pchl_{id}e in methanol, the excited state dynamics, as recorded via fluorescence, result in a 50 ps time constant that seems to correspond to the 300 ps process in the TA data. The reason for this difference may lie in the difficulties associated with fitting multi-exponential dynamics in a very wide spectral interval, but also in the fact that the Streak experiment reveals the dynamics of the fluorescence emission, whereas the TA experiment reveals the additional recovery of the depleted GS and dynamics of the ESA. In the current case, where the radiative emission is quenched during the lifetime of the excited state, this may lead to slightly deviating results, if one considers inhomogeneity and cooperative effects: chromophores having stronger oscillator strengths (less of the ICT character mixed

in the excited state) experience more quenching, resulting in shorter lifetimes. These would dominate the fluorescence experiment, whereas quenched Pchlide molecules (having more ICT character) experience slower dynamics and will contribute equally with the less-quenched states to the TA. The description of such inhomogeneities, or cooperative effects, would require a more elaborate analysis than presented here. Our results on the excited state dynamics of Pchlide are summarized in the energy level diagram depicted in figure 5.6.

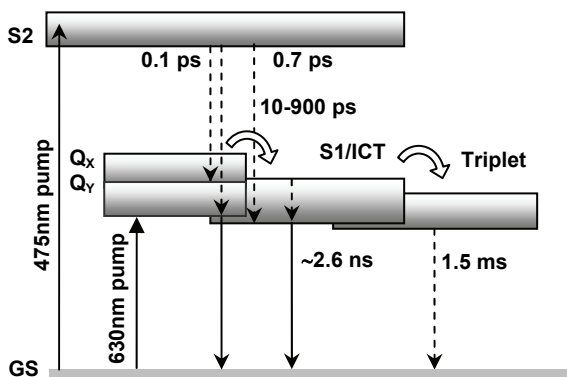


Figure 5.6. Energy level diagram of Pchlide excited state relaxation processes upon Soret excitation at 475 nm and direct excitation of the Q_Y band at 630 nm. Dashed arrows indicate non-radiative transitions, solid arrows indicate radiative transitions, decay rates are shown for solvation in THF.

5.4.4. Comparison with previously reported Pchlide studies

A number of studies to characterize the excited state dynamics of Pchlide in a variety of solvents (methanol, acetonitrile, cyclohexane) have been published in the last few years⁽⁸³⁻⁸⁶⁾. Transient absorption difference spectra recorded upon 600 nm excitation, show a similar ~4 ps blue-shift of the negative transient absorption signals to those reported here, in acetonitrile but not in methanol⁽⁸⁶⁾. Earlier fluorescence Streak experiments did not resolve this blue-shift, probably because the IRF was too long⁽⁸⁴⁾. In Dietzek *et al*⁽⁸⁶⁾ the blue-shift was tentatively assigned to vibrational cooling. This is confirmed in the present work by the comparison of sets of spectra obtained at two excitation wavelengths, which firmly show that a gain and a blue-shift of emission on the sub-ps and ps timescales appears only upon excitation in the Soret. Hence, this is a consequence of a relatively slow S2→S1 transition,

occurring in conjunction with vibrational cooling. Note, that the faster, sub-ps components reported here, were not resolved in the earlier studies⁽⁸³⁻⁸⁶⁾. The multiphasic (2.5 ps, 26 ps and 250 ps) decay of signal in methanol reported upon excitation at 630 nm⁽⁸⁵⁾ resembles our data in methanol. However, the previously proposed branched model, where 60% of the excited state in 22-27 ps decays via a reactive pathway to a blue charge-transfer state SICT in polar solvents and the remaining 40% of the excited molecules populate a non-reactive red emissive S1 state⁽⁸⁵⁾, is not supported by our mid-IR data. The absence of decay in the mid-IR difference absorption signals up to 3 ns demonstrates that the solvation of the ICT state does not lead to the loss of the excited state population, but to a shift of the excited state potential. This results in a red-shift and quenching of the fluorescence emission and dynamics of the ESA. The time-resolved fluorescence and transient absorption signals in both the visible and mid IR regions can be effectively described with a simple sequential mechanism, which accounts for a slower population of the S1/Q_Y state upon excitation in the Soret. According to this model, multiphasic quenching of the excited state emission occurs via solvation of the S1/ICT state and the subsequent population of the triplet state occurs with a yield of 0.231. This result is in full agreement with the theoretically proposed ICT state of the isolated excited Pchl_{ide}⁽⁴¹⁾ and for Pchl_{ide} solvated in methanol⁽⁴¹⁾. As our experiments show, the ICT state is formed regardless of the H-donating properties of the solvent and is therefore, an intrinsic characteristic of Pchl_{ide} (otherwise the multi-exponential quenching in THF would not be observed).

Importantly, our mid-IR data has now highlighted important structural features of Pchl_{ide} and the organization of the surrounding solvent molecules, via shifts in the vibrational frequencies of the C=O keto group of the cyclopentanone ring in Pchl_{ide}. The presence of two site-specific solvation patterns in methanol, and only one pattern in THF, appears to support the previous TDDFT calculations⁽⁴¹⁾. The combined observations in the mid-IR region of a downshift of the keto mode with the solvation of the ICT state in methanol, suggests the involvement of a dynamic H-bond at the keto site during the creation and solvation of the ICT state. As the more polar and H-bonding solvent methanol is a better mimic of the protein environment it is possible that the C13¹=O site might be also important for the enzymatic photoreduction of Pchl_{ide}. Previously it has been demonstrated that the activity of the enzymatic photoreduction is eliminated by alteration in the chemical structure of the cyclopentanone ring E⁽⁷⁾. The modifications in the C13¹=O groups led to loss of the Pchl_{ide} ability to form tautomers (strongly H-bonded state), and

1 Note, that according to Dietzek *et al.* the population of a triplet state from the vibrationally cold S1 state occurs on the timescale of 3.5 ns and with a very high estimate of 0.85, whereas the triplet yield with respect to the entire excited state population is 0.34, not too dissimilar from our 0.23 estimate. (85) B. Dietzek, S. Tschierlei, G. Hermann, A. Yartsev, T. Pascher, V. Sundstrom, M. Schmitt, and J. Popp, "Protochlorophyllide *a*: A Comprehensive Photophysical Picture". *Chemphyschem*, 2009, **10**(1)

thus it was suggested that the protonation of the C13¹=O is probably necessary for the photoreduction⁽⁷⁾. It is also important to note that the branched excited state dynamics with fast deactivation of the ICT state⁽⁸³⁻⁸⁶⁾, is likely to result in different routes for the enzymatic photoreduction of Pchlide than the sequential dynamics.

5.4.5. Relevance for the catalytic reaction mechanism in the POR enzyme

Following light excitation of Pchlide bound to the POR enzyme, Pchlide is efficiently reduced to Chlide⁽⁵⁾. Its high excited state reactivity and intrinsic ability to form an ICT state are likely to be important elements for this enzymatic reaction. The binding of Pchlide to the protein causes a 10 nm red-shift in the absorption spectrum. In addition, in fluorescence line narrowing experiments (unpublished data) we found that the keto carbonyl group of Pchlide is downshifted by 50 cm⁻¹ relative to the unbound state, which is an indication of strong hydrogen bonding between Pchlide and protein residues, stronger than the hydrogen bond with methanol. The first intermediate⁽⁵²⁾ in the catalytic cycle of POR is an excited state, formed with effective rates of ~300 ns⁻¹ and ~3.7 ns⁻¹, that emits at 675 nm, denoted as I675*. Clearly, the formation of such a state is not observed when the Pchlide molecule is dissolved in THF, methanol or buffer, which confirms that this is an enzyme-specific reaction that is only possible in the ternary enzyme-substrate complex. Therefore, the I675* intermediate is of a different nature than the solvated ICT and H-bond state, formed in the solvents studied here. However, the enzyme needs to be activated via a conformational change, before Pchlide reduction can take place⁽⁵²⁾. Before this activation, the Pchlide molecule shows a progressive loss of emission⁽⁵²⁾ with time constants similar to those found in this work. It is possible that either the ICT state, or the triplet state, is involved in triggering the protein conformational change that is required before the actual catalysis⁽⁵²⁾.